J. Fluid Mech. (1982), *vol.* 117, *pp.* 1–26
Printed in Great Britain

Concentration fluctuations and fluxes in plumes from point sources in a turbulent boundary layer

By J. E. FACKRELL AND A. G. ROBINS

Marchwood Engineering Laboratories, Central Electricity Generating Board, Marchwood, Southampton, SO4 4ZB, U.K.

(Received 21 January 1981 and in revised form 9 June 1981)

Measurements have been made of concentration fluctuations and turbulent fluxes for two passive plumes from an elevated and a ground-level source in a turbulent boundary layer. For the concentration fluctuations, results are presented for the variance, the intermittency, peak values of concentration, probability-density functions and spectra. The balance of terms in the variance transport equation is examined, as is the overall level of fluctuations along the plume. It is shown that most of the production of fluctuations occurs very near the source. Then, the level of fluctuation decays, roughly in accordance with a balance between advection and dissipation. For the turbulent fluxes of concentration, results are presented for the vertical and lateral fluxes, with the associated behaviour of the vertical and lateral eddy diffusivities. The balance of terms in the transport equations for the fluxes is examined. The essential differences between vertical diffusion from ground-level and elevated sources and between near-field and far-field behaviour are shown to be due to the relative importance of the advection and diffusion terms in these equations.

1. Introduction

In recent years, owing to an increasing interest in environmental problems, considerable attention has been focused on means of predicting concentration levels downwind of point sources in turbulent boundary layers. In practice, predictions are often required for dispersion in complicated flow fields influenced by buoyancy effects, buildings, topography, etc. By restricting consideration to a passive release into a known boundary-layer flow, problems associated with the behaviour of the flow and with source momentum and buoyancy are avoided. Yet, even in this simple case, many aspects of the dispersion, especially the behaviour of the concentration fluctuations and fluxes, are poorly understood. Despite this, the recent tendency has been to attempt to overcome the inherent flaws in the simple gradient-transfer approach to dispersion modelling by moving to higher-order models, i.e. modelling the transport equations for the fluxes themselves (e.g. Lewellen & Teske 1976; Harter *et al.* 1980). There has been little experimental evidence to guide this work and it has been clear for some time that thorough experimental studies of plume structure and development are required. It is hoped that the present paper will go some way towards fulfilling this need.

A natural development of higher-order models lies in the prediction of concentration fluctuations. This is a problem of considerable importance in assessing the likely effects of air pollutants on plants and animals or the hazard from releases of toxic or

inflammable gases and in studying some of the chemical processes within plumes. Some of the initial attempts at both predicting concentration fluctuations (Csanady 1967; Thomas 1979) and measuring fluctuations in ground-level plumes (Robins & Fackrell 1979) have again emphasized the need for thorough experimentation, particularly for elevated emissions.

Studies of fluctuating concentration have been hampered by a lack of suitable instrumentation; though, recently, successful investigations have been undertaken using light-scattering techniques (Gad-el-Hak & Morton 1979; Birch *et al.* 1978) and heat tagging (Belorgey, Nguyen & Trinite 1979). In the present work, a modified flame-ionization detector was used, which, in conjunction with a crossed hot wire, enabled the majority of the terms occurring in the transport equations for the concentration fluxes and fluctuations to be measured.

There is an important distinction to be made between elevated and ground-level sources. For a ground-level source the vertical scale of the plume always exceeds that of the turbulence, so that vertical dispersion progresses in a 'far-field' manner and, consequently, can be described adequately by simple gradient-transfer or similarity arguments. This is not the case for an elevated source or, indeed, for lateral spreading from sources at any height. It has also been found experimentally (Robins & Fackrell 1979) that many of the statistical quantities associated with a ground-level plume exhibit an approximately self-preserving form, at least until the plume begins to fill the boundary layer. An elevated plume can also be self-preserving whilst it remains fully elevated, but at some stage in its growth the influence of the ground will begin to change its structure until, eventually, it comes to resemble a ground-level plume. In the present work, a ground-level source and a source at $0{\cdot}19H$ (where H is the boundary-layer height) were studied. The elevated source height was chosen as being roughly representative of many full-scale emissions, and because it enabled examination of the change in plume structure from a fully elevated one towards a ground-level form within the downstream distance available in the wind tunnel.

In the present paper experimental observations of source-size effects will be described and their relevance to the formulation of higher-order transport-equation models discussed. A detailed analysis of the effects of source size on concentration fluctuations and their prediction by a statistical analysis of turbulent diffusion will be reported separately (Fackrell & Robins 1981). For the ground-level source the present work has a general validity, as source size is not a significant factor in ground-level plumes. This is not true of elevated emissions, and concentration-fluctuation data are specific to the particular source sizes studied; though this comment does not apply to the measurements of concentration fluxes.

Attention will not be focused on the behaviour of the mean concentration field any more than is necessary, but rather on the fluxes and fluctuations, as it is in these areas that the main virtues of the work lie. Indeed, there are virtually no published studies of these topics as they relate to dispersion of passive contaminants in turbulent flows. Detailed investigations have been undertaken in jet and wake flows (Freymuth & Uberoi 1973; Birch *et al.* 1978). However, these are somewhat different problems (the extents of the turbulence and concentration fields being similar) and the most relevant previous studies are those of Becker, Rosensweig & Gwozoz (1966), in a pipe flow, and Gad-el-Hak & Morton (1979), in grid-generated turbulence. The present work, which is in many respects more detailed, concerns dispersion in a turbulent

boundary-layer flow. Because the main concern is in providing experimental information to aid prediction techniques, results will be presented solely in terms of dispersion in the laboratory boundary layer, with no attempt to compare with full-scale measurements. However, much of the paper should be of direct relevance to short-range dispersion in the neutral atmospheric boundary layer, at least for full-scale quantities averaged over fairly short times, of a few minutes to about one hour. In addition, both the flux and fluctuation results should be of wider interest, with, for example, some application to combusting or reacting flows.

2. Experimental techniques

The experiments were undertaken in the Marchwood Engineering Laboratories' $24 \times 9{\cdot}1 \times 2{\cdot}7$ m open-circuit wind tunnel. A 1·2 m high boundary layer was generated in the tunnel by the method of Counihan (1969). Plumes from sources at two different heights were studied: $z_s/H = 0{\cdot}19$ and 0. For the majority of the study the ground-level source (GLS) consisted of a horizontal tube, 15 mm in diameter, aligned with the flow and placed just above the roughness elements of the floor. It emitted at the average velocity of the flow over its height. The elevated source (ES) was an 8·5 mm diameter tube, similarily arranged, emitting at the velocity at its height. In order to investigate the importance of source size, a variety of sources were used, their diameters ranging from 3–35 mm; all being small compared to the boundary-layer height. The source gas consisted of a neutrally buoyant mixture of propane and helium, the former being used as a trace gas for concentration measurement.

Fluctuating concentration measurements were made with a modified flame-ionization detector system. A detailed description of this system, including its use in conjunction with DISA crossed hot wires to obtain the fluxes, is given by Fackrell (1980). The -3 dB point of the frequency response of the concentration-sensing probe was about 300 Hz. As shown later, this allowed the most energetic fluctuations and some of the inertial subrange to be measured, although excluding, of course, fine-scale structure. Instrument sensor dimensions cannot necessarily be ignored and, in the present case, effective sample diameters, normal to the flow, were about 1 mm; cf. a Kolmogorov length scale of 0·1 mm. However, for the present instrumentation, the above-mentioned frequency response actually sets the limit of resolution, since it is equivalent to a streamwise fetch greater than the sample diameter. Signals from the concentration probe and the hot wires were all processed digitally to obtain the required statistical quantities, with enough samples being taken to achieve good repeatability. No corrections for high turbulence levels have been applied to the hot-wire results, since turbulence levels were fairly low, resulting in errors of less than 10% in the shear stress. As illustrated by results presented later, the accuracy of concentration and flux measurements is probably similar to this, except where the values are small, when the errors will be greater.

3. The velocity field

The boundary layer used in these experiments was artificially thickened using the method evolved by Counihan (1969). A detailed discussion of the structure of such boundary layers is given by Robins (1979), from which it follows that the flows are

$H(m)$	z_0/H	u_*/U_e
1·2	$2{\cdot}4 \times 10^{-4}$	0·047

TABLE 1. Boundary-layer characteristics

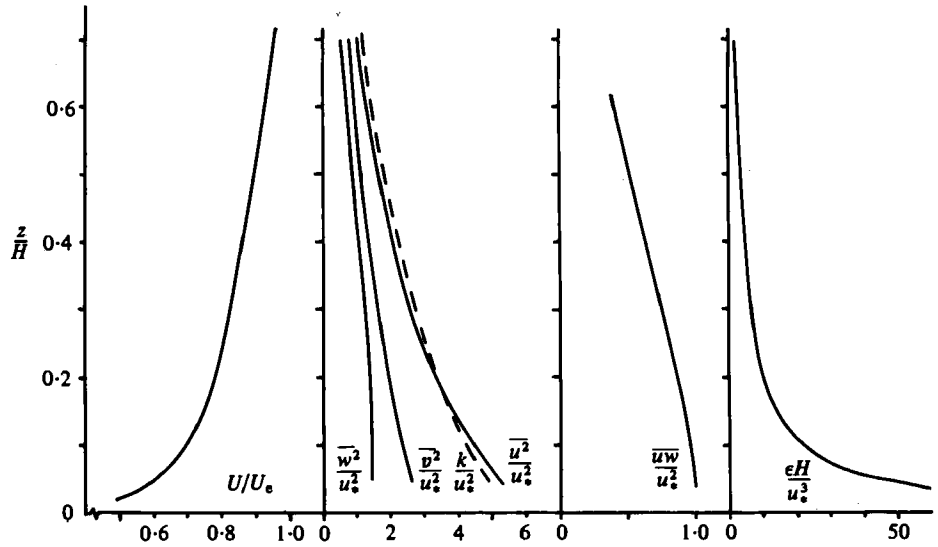

FIGURE 1. Vertical profiles of mean velocity, normal and shear stresses, turbulent energy and dissipation rate. The curves shown are an average through many experimental points.

indistinguishable from naturally grown boundary layers beyond a certain distance from the devices used for thickening. The sources in the present case were located to satisfy this requirement and, consequently, the flow field may be assumed to be an ordinary, equilibrium, zero-pressure-gradient boundary layer. Some characteristic properties are given in table 1. U_e is the mean velocity at the boundary-layer edge, u_* is the friction velocity, and z_0 is the roughness length, such that the log law is $U \doteq (u_*/k) \ln\{z/z_0\}$, where z is the vertical distance above the zero-velocity height and k is von Kármán's constant. As diffusion measurements were restricted to a relatively short overall downstream fetch, about $8H$, boundary-layer growth can be neglected. Figure 1 presents vertical profiles of mean velocity U, shear and normal stresses uw, u^2, v^2, w^2, turbulent energy

$$k = \tfrac{1}{2}(\overline{u^2} + \overline{v^2} + \overline{w^2}),$$

and energy dissipation rate ϵ. Note that the forms of these profiles are consistent with those of naturally grown boundary layers. For comparison with concentration fluctuation spectra presented later, figure 2 presents the spectrum of longitudinal turbulence ϕ, in the form $\phi/H\overline{u^2}$ against Hk_1, where $k_1 = 2\pi f/U$ and f is frequency. Results are shown for two heights and three flow speeds. Note in particular that the inertial subrange appears to extend over one to two decades, being slightly smaller at the lower flow speeds. Most of the measurements in this paper were made at a free-stream speed of $4\,\mathrm{m\,s^{-1}}$.

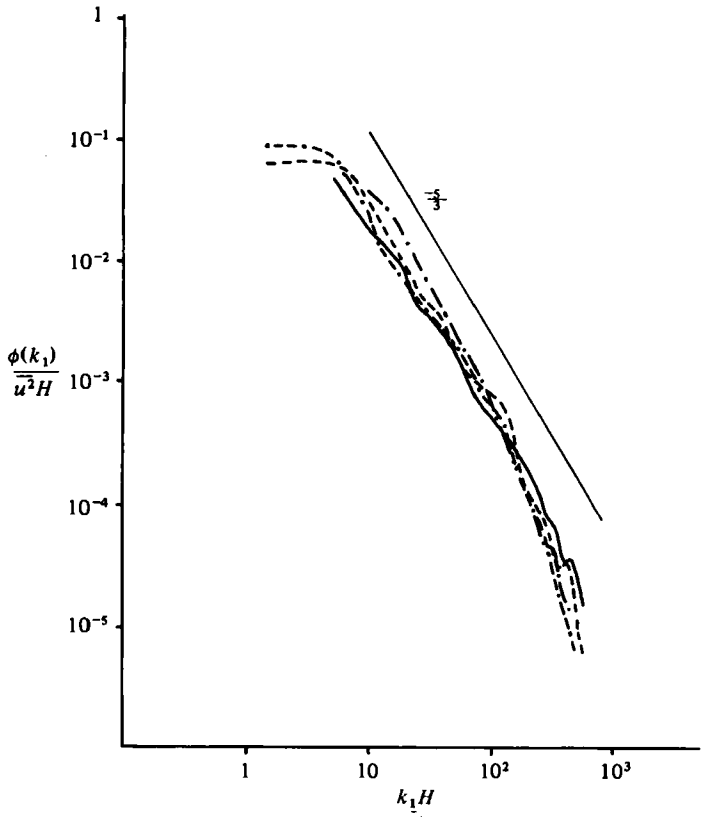

FIGURE 2. Wavenumber spectrum of longitudinal velocity fluctuations ($k_1 = 2\pi f/U$): ——, $U_e = 4$ m s^{-1}, $z/H = 0{\cdot}083$; – – –, 2, 0·083; – · –, 1, 0·083; – – · – –, 2, 0·330.

4. Mean-concentration field

Mean-concentration data may be used to evaluate the usefulness of the classical theories of turbulent diffusion (see e.g. Pasquill 1974) and their later developments (Hunt & Weber 1979) in boundary-layer flows, rather than in the idealized conditions required by the theories. Such matters have been discussed in an earlier paper (Robins & Fackrell 1979) and will be considered in greater depth in a future paper, including the effects of source height from 0 to 0·5H. For present purposes the mean concentration fields will only be described in sufficient detail for their use in the main part of this paper, which is the consideration of the concentration fluxes and fluctuations. Figure 3 shows the variation of maximum mean concentration C_m with downstream distance for ground-level (GLS) and elevated (ES) sources. For the GLS, the maximum at any downstream station is always at ground level. For the ES it approaches the ground, being at ground level for the furthest downstream position; ground-level concentrations C_0 are plotted separately. Also shown are the vertical- and lateral-plume half-widths δ_z and δ_y, where the half-width is the distance in which the maximum concentration falls to half its value. The lateral half-widths are roughly the same for both sources and increase proportionally to x near the source and $x^{\frac{1}{2}}$ far downstream, in agreement with statistical theory. The ES vertical half-width shows similar behaviour, but the GLS vertical half-width, being consistent with similarity theory,

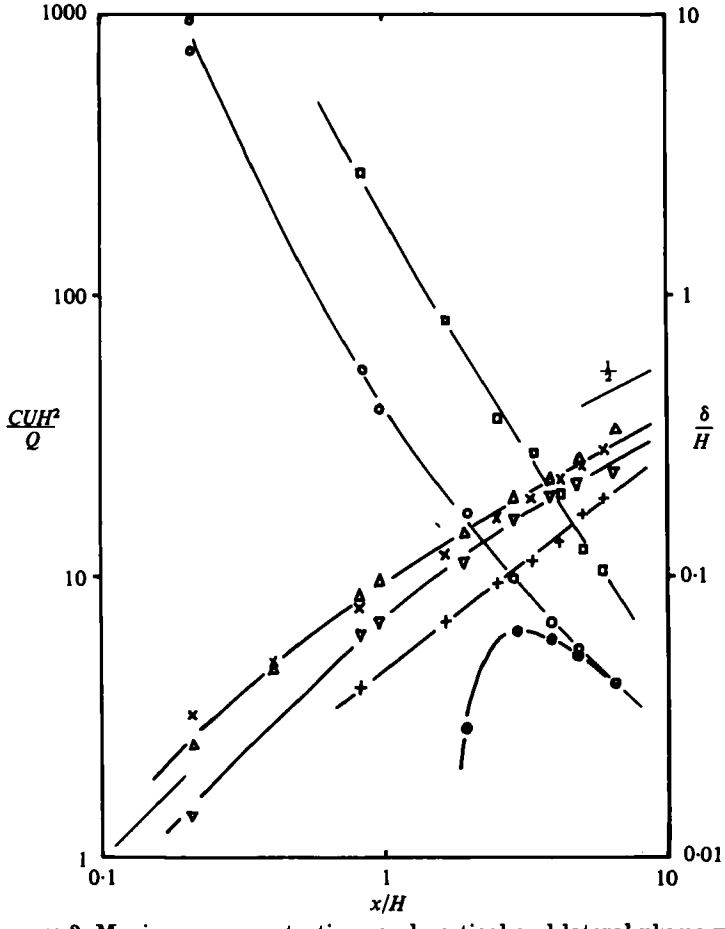

FIGURE 3. Maximum concentrations and vertical and lateral plume widths: □, C_m, GLS; +, δ_z; ×, δ_y; ○, C_m, ES; ●, C_0; ▽, δ_z; △, δ_y.

appears to have a power-law dependence, approximately $x^{0.75}$, over all the distance covered by the results. The ES vertical half-width is significantly larger than the GLS one.

Figure 4(*a*) shows vertical profiles of mean concentration for the ground-level source in a self-preserving form. This form is described closely by the empirical relation given by Robins (1978) for ground-level source measurements,

$$C = C_0 \exp\{-0{\cdot}693(z/\delta_z)^s\}, \tag{1}$$

although $s = 1{\cdot}5$ gives the best fit to the present data, whilst $s = 1{\cdot}7$ gave a better fit to the earlier results, obtained in a much rougher boundary layer ($z_0/H = 0{\cdot}0022$). This variation of s with roughness is, in form, consistent with the predictions of Hunt & Weber (1979).

In figure 4(*b*) are shown vertical profiles of mean concentration at various stations along the plume from the elevated source. The origins for successive profiles are offset to the right for clarity. The curves are profiles obtained using a reflected Gaussian model:

$$C(z) \sim \{\exp(-0{\cdot}693(z+z_s)^2/\delta_z^2) + \exp(-0{\cdot}693(z-z_s)^2/\delta_z^2)\},$$

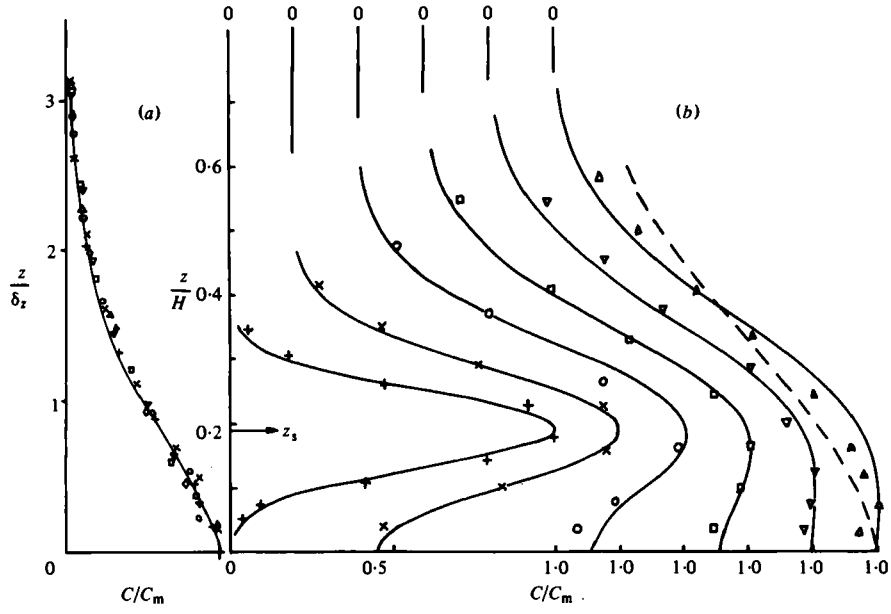

FIGURE 4. Vertical profiles of mean concentration, $y/H = 0$. (*a*) GLS: ◇, $x/H = 0{\cdot}83$; □, 1·67; △, 2·50; ○, 3·33; ▽, 4·17; ×, 5·00; +, 5·92; ——, equation (1) with $s = 1{\cdot}5$. (*b*) ES: $x/H =$ 0·96; ×, 1·92; ○, 2·88; □, 3·83; ▽, 4·79; △, 6·52; ——, reflected Gaussian model.

which can be seen to give a reasonable fit to the experimental points. In fact, the vertical half-widths given for the elevated source in figure 3 are the half-widths of the individual Gaussian curves giving the best fit to the experimental profiles. This results in a straightforward growth of vertical spread with distance, whereas the spread, say as measured upwards from the observed maximum concentration, actually develops in a rather complex manner whilst the plume is in transition from an elevated to a ground-level form. Of course, the Gaussian profile is not an ideal description of a ground-level plume, so that the derived plume spread, whilst useful for some practical purposes, is not exact, which simply reflects the error implicit in Gaussian plume models. Up to $x/H = 1$ the plume is fully elevated and the profiles are very close to Gaussian; thereafter the development from the elevated Gaussian profile to one reminiscent of a ground-level source can be seen clearly. For comparison with the furthest downstream result, the self-preserving ground-level profile (1) is shown as a dashed line, arranged so that $C/C_m = 0{\cdot}5$ at the same height as in the measured profile. The plume begins to touch the ground before $x/H = 1{\cdot}92$ (or $x/z_s = 10$) and the maximum ground-level concentration occurs at about $x/H = 3{\cdot}3$; yet by $x/H = 6{\cdot}5$ there is still some development needed before a GLS profile is obtained.

For both ground-level and elevated sources, the lateral profiles at all stations were closely Gaussian in nature, and the lateral-plume half-width δ_y was found to be constant with height at any station, within the experimental error of about $\pm 5\,\%$.

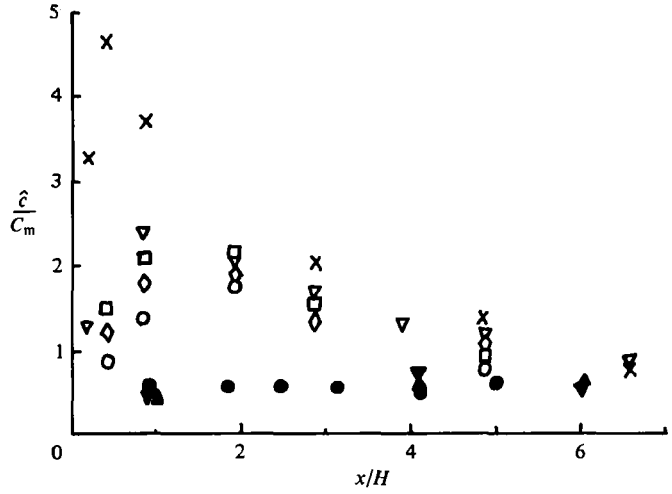

FIGURE 5. Relative intensity of fluctuations. GLS: ▲, source diameter d_s = 3 mm; ▼, 9; ●, 15. ES: ×, d_s = 3 mm; ▽, 9; □, 15; ◇, 25; ○, 35.

5. Concentration fluctuations

5.1. *The variance*

It is well-established on theoretical grounds that the observed statistics of a fluctuating concentration field are dependent upon both sensor dimensions and source conditions (Durbin 1980; Chatwin & Sullivan 1979). For the present work, the former were fixed, as described briefly in § 2 and, in more detail, in Fackrell (1980), whilst the latter were allowed to vary and, for a range of source sizes, the axial variations of maximum mean-square fluctuations were obtained. Figure 5 shows the behaviour of the relative intensity of concentration fluctuations, plotted as $\hat{c}/C_m$, where $\hat{c}$ is the maximum r.m.s. and C_m the maximum mean at any downstream position. For the elevated source the effects of source size are large, whereas for the ground-level source they are not distinguishable from the experimental scatter. For the elevated source an analysis in terms of a fluctuating- (or meandering-) plume model (Gifford 1959), using the results of Hay & Pasquill (1959) and Smith & Hay (1961) to determine relevant plume scales, shows meandering to be the main source of concentration fluctuations (Fackrell & Robins, 1981). This work shows that the appropriate measure of source size, in so far as the fluctuations are concerned, is the ratio of diameter to turbulence lateral (or vertical) integral scale (a conclusion reached by Durbin 1980). Thus it was found that the overall maximum intensity varies like $\Delta^{-0.4}$, where Δ is the diameter-to-integral-scale ratio, whereas the downstream position at which this maximum occurs behaves as $\Delta^{0.7}/\sigma_\theta$, where σ_θ is the lateral intensity of turbulence. As meandering is the major source of concentration fluctuations in an elevated plume (which follows from the fact that the dimensions of the plume are initially less than the turbulence scales) it is to be expected that much lower levels of fluctuation, and smaller effects of source conditions, are to be found in plumes from ground-level sources. That there should be no significant source-size effect is not obvious, though it does indicate that the behaviour of the lateral turbulence scales near the surface is worthy of study; likewise characteristic times associated with dispersion in the close vicinity of roughness elements.

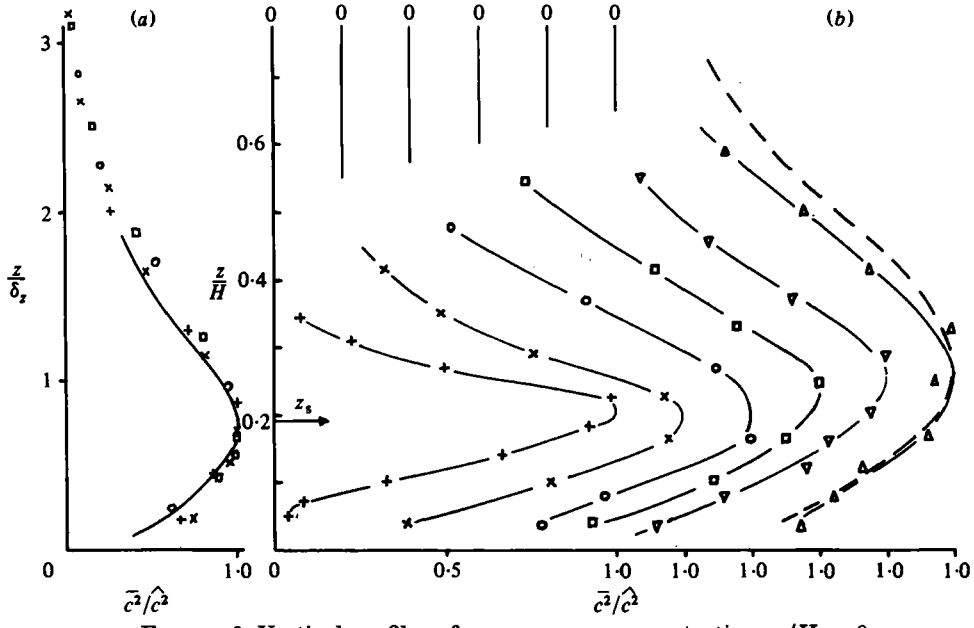

FIGURE 6. Vertical profiles of mean-square concentration, $y/H = 0$. Symbols as in figure 4.

In order to consider the development of concentration fields in more detail attention was restricted to two source sizes, as given in §2. For the GLS, the vertical profiles of mean-square fluctuating concentration are approximately self-preserving, as shown in figure 6(*a*); the curve being the average of the earlier results of Robins & Fackrell (1979) obtained in a different boundary layer. The maximum of $\overline{c^2}$, $\hat{c}^2$, occurs at $z/\delta_z \simeq 0{\cdot}75$, which is roughly the position of maximum production of $\overline{c^2}$ on the centre line. Both production and advection of the concentration fluctuations decrease near the ground (see later) and this causes $\overline{c^2}$ to tend towards zero at the ground, although as it was not profitable to explore this limit by making measurements amongst the roughness elements it cannot be said that a zero value is indeed reached. The condition of zero (or very small) transfer to the ground ($\partial C/\partial z \to 0$, $z \to 0$) appropriate to most plume situations, makes the behaviour near the ground in this and other ways quite different from the situation more usually considered of high (heat or mass) transfer to or from the boundary. It follows that modelling approximations that have been made in the latter case, assuming local equilibrium near the wall, cannot necessarily be applied to plume modelling.

Vertical profiles of $\overline{c^2}$ for the ES are presented in figure 6, and as in figure 4 the origins of successive profiles are offset to the right. The curves in this figure are just empirical fits drawn in for clarity of presentation and do not represent any particular functional form. However, although not shown in the figure, elevated profiles for $x/H < 1$ are at least as close to Gaussian as the mean profiles. Indeed, the first two profiles shown are closely similar to the corresponding mean profiles; it is only the later profiles which show a clear divergence between the two, with the final $\overline{c^2}$ profile tending towards the self-preserving form found for the GLS. The height of the

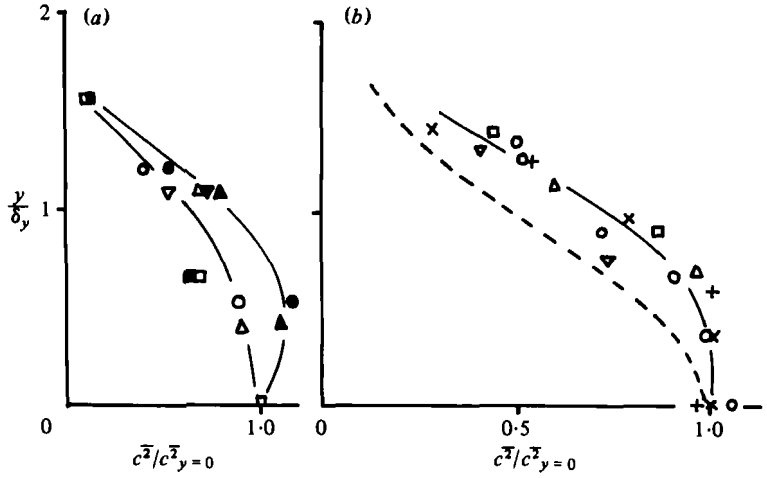

FIGURE 7. Lateral profiles of mean-square concentration. (*a*) GLS: ●, $x/H = 5{\cdot}92$, $z/\delta_z = 0{\cdot}5$; ○, 5·92, 1·5; ▼, 4·17, 0·5; ▽, 4·17, 1·5; ▲, 2·5, 0·5; △, 2·5, 1·5; ■, 0·83, 0·5; □, 0·83, 1·5. (*b*) ES: – – –, Gaussian, other symbols as in figure 4(*b*).

maximum in mean concentration falls towards the ground with increasing fetch whilst that of the maximum in $\overline{c^2}$ tends upwards.

The lateral variation in $\overline{c^2}$ is illustrated for both sources in figure 7. It is deduced in Robins & Fackrell (1979) that the maximum production of $\overline{c^2}$ for a GLS should occur on the centre line above $z/\delta_z \simeq 1$, but off the centre line below this. A similar behaviour is shown by the measured values of $\overline{c^2}$ as illustrated in figure 4(*a*), where, apart from a value at $x/H = 0{\cdot}83$, the results at $z/\delta_z = 0{\cdot}5$ show a maximum off the centre line, whilst those at $z/\delta_z = 1{\cdot}5$ decrease away from the centre line. Figure 7(*b*) presents the lateral variation in $\overline{c^2}$ for the ES at the height of the maximum value of $\overline{c^2}$ at each station. The lateral profiles are roughly similar at the different downstream positions and the profile shape is broader than the Gaussian curve of the mean concentration. Over the downstream distance examined, there is less variation of the lateral profile with height for the ES, although close examination of the results suggests that the profile is slightly broader lower down in the plume.

5.2. *Probability-density functions*

Probability-density functions $p(c)$ for the ES measured on the centre line at $x/H = 4{\cdot}79$ at various heights are given in figure 8 in the non-dimensional form $c'p$ versus $(c - C)/c'$, where C is the mean concentration, c' the r.m.s. At this position, the plume is being greatly influenced by the presence of the ground. The distribution obtained near the ground show a tendency towards a Gaussian form. In fact, the best fit to the distributions near the ground was obtained with a 3-parameter lognormal distribution. Higher in the plume the p.d.f.s obtained are of a form which might be described as 'exponential-like'. Indeed, the exponential distribution, $p(c) = A\,e^{-Bc}$, suggested by Csanady (1967) and Barry (1970), does provide a good fit to the distribution, except near $c = 0$. The rapid increase in value near $c = 0$ is a genuine effect and not due to noise on the measurements; the small effect of noise is indicated by the very low values obtained for points just less than $c = 0$. Nearer to the source, with the plume

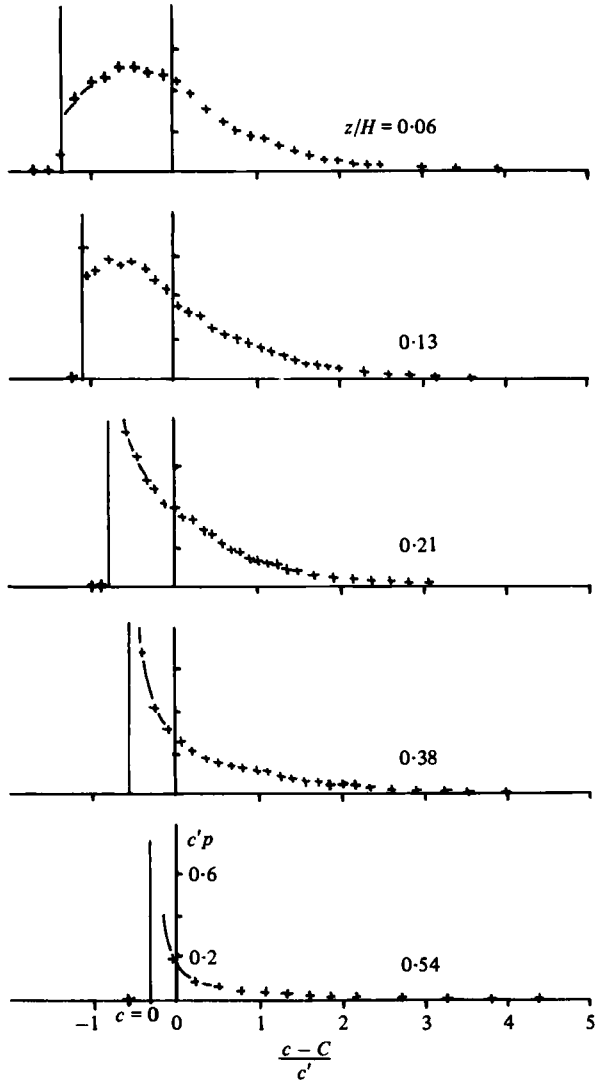

FIGURE 8. Probability-density distributions, $x/H = 4{\cdot}79$, $y/H = 0$, ES.

fully elevated, the same type of distribution is obtained at all positions in the plume. Good fits to these distributions are obtained with a power law $p(c) = \alpha c^{-\beta}$; a form given by the fluctuating Gaussian-plume model of Gifford (1959). Its agreement with the data suggests that most of the fluctuations contributing to the p.d.f. arise from the meandering of the instantaneous plume. Further downstream than shown the distributions near the ground become very close to Gaussian; only those higher in the plume remain 'exponential-like'. Distributions obtained for the GLS near to the source, $x/H < 3$, are similar to those shown in figure 8, whereas further downstream a Gaussian form is found near the ground (see e.g. Robins & Fackrell 1979).

O'Brien (1978) has obtained similarity solutions of a model p.d.f. equation, which under certain assumptions can give a Gaussian distribution near the centre of a plume

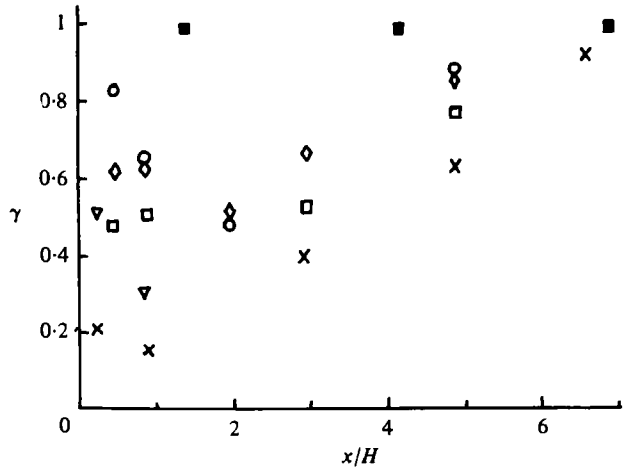

FIGURE 9. Plume-axis $(x, 0, z_s)$ intermittency factors. ES: symbols as in figure 5. GLS: ■, Robins & Fackrell (1979).

and an exponential distribution at the edges. The assumptions made in obtaining the exponential distribution imply that the small-scale mixing process at the edge of the plume is very rapid and dominates the distribution of the concentration in this region. An examination of the low-noise signal from the FID on an oscilloscope shows that, in regions where exponential-type distributions are obtained, a large number of short, small excursions from $c = 0$ are found with relatively fewer much larger, longer excursions. This suggests a complex 'wispy' structure near the edge of the plume, again implying rapid small-scale mixing.

The intermittency factor γ, defined as the proportion of time for which $c > 0$, can be obtained from p.d.f.s by integrating over all $c > 0$. Zero values of concentration contribute a delta function to the p.d.f. at $c = 0$, with area such that the total integral is 1. Alternatively, γ can be obtained by setting some small threshold value of concentration. In either way of obtaining γ, the resulting values have a small degree of uncertainty due to noise on the zero-concentration signal.

The effect of source size on the plume axis $(x, 0, z_s)$ intermittency level is shown in figure 9; these results, together with the variance data of figure 5, show the importance of plume meandering near to the elevated source. For small sources the rate of growth of the mean plume considerably exceeds that of the 'instantaneous' plume and, although at the source $\overline{c^2} = 0$ and $\gamma = 1$, the potential for a rapid growth in concentration fluctuations clearly exists. Extreme examples of the source-size effects are demonstrated in work of Jones (1979), who observed very low intermittency factors near a small source about 1 m above the surface in the atmosphere, and Gad-el-Hak & Morton (1979), who found an intermittency factor of unity on the axis of a plume from a relatively large source in grid-generated turbulence. Profiles of intermittency factor for the ES, derived from the p.d.f.s, are given in figure 10. The absolute value of γ is dependent on source size, but the overall shape of the curves at different positions is similar for all the source sizes examined. γ increases with downstream distance, especially near the ground, where it tends towards a value of unity; and the lateral variation shows a decrease with distance from the centre line. Intermittency distributions for a GLS, given in Robins & Fackrell (1979), show a γ value of 1 near the

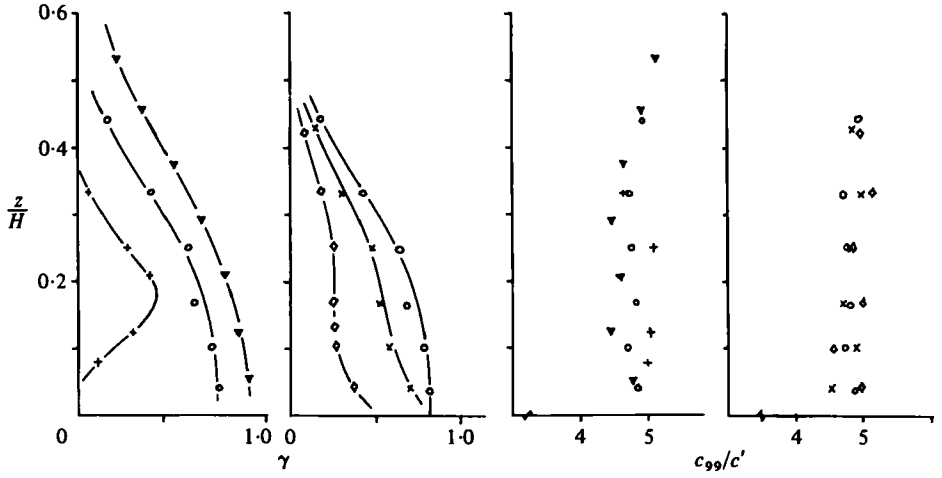

FIGURE 10. Intermittency factor and peak values of concentration, ES: +, x/H = 0·96, y/δ_y = 0; ○, 2·88, 0; ▽, 4·79, 0; ×, 2·88, 0·67; ◇, 2·88, 1·37.

ground on the plume centre line and an approximately self-preserving form, although there is some indication that γ values are higher further out in the plume as the distance from the source increases. This may be a reflection of the increasing ratio of plume width to lateral turbulence scale.

Because the concentration is exactly zero outside the plume, neglecting any noise on the signal, it is possible, knowing γ, to derive statistical quantities conditioned to include contributions only when the plume is present ($c > 0$). For example the conditioned variance is related to the overall one by

$$\overline{c_c^2} = \frac{\overline{c^2}}{\gamma} + \frac{C^2(\gamma - 1)}{\gamma^2}.$$

However, there is not a great deal to be gained by this. What one would really like to obtain are statistical quantities measured at a position fixed relative to the centre of the instantaneous plume. The above conditional technique does not provide this, since contributions with $c > 0$ will be obtained for many different positions in the instantaneous plume.

Another quantity of interest which can be derived from the p.d.f. is the peak concentration, here defined as the value which is exceeded only 1 % of the time, c_{99}. Values of c_{99} measured for the GLS are given in Robins & Fackrell (1979), where it is shown that, despite the wide range in p.d.f. shapes, the quantity c_{99}/c' is remarkably constant over most of the plume, with an average of about 4·5. Figure 10 gives results for the ratio c_{99}/c' for the elevated source and, again, it is shown to be fairly constant at about 4·5–5 (N.B., c_{99} is an absolute value, not measured relative to the mean). It is worth mentioning that similar results for this ratio have been obtained in all our measurements in plumes, even those with buoyancy and momentum (e.g. Fackrell 1978).

5.3. *Spectra*

Power spectral measurements of the concentration fluctuations have been made for both sources. These measurements were made at a free-stream speed of 2 m s^{-1}, with some repeated at 4 m s^{-1} to confirm that the frequency response of the measuring

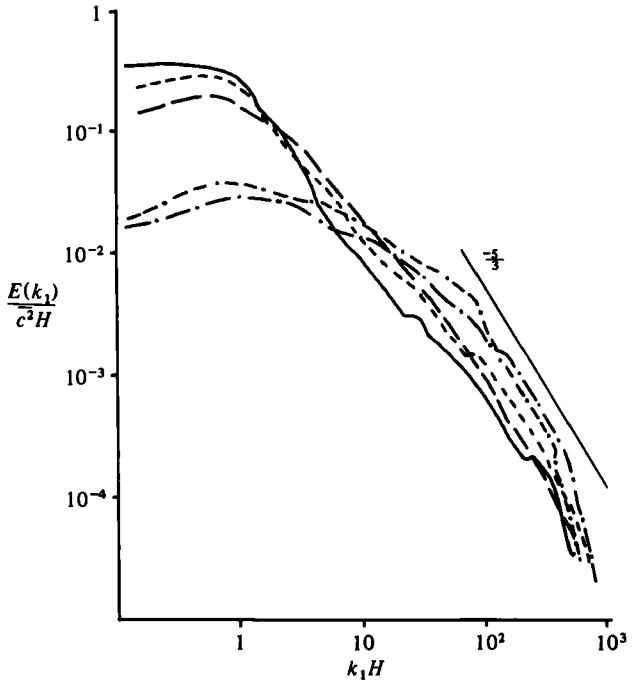

FIGURE 11. Spectra of concentration fluctuations, $y/H = 0 (k_1 = 2\pi f/U)$: ——, GLS, $x/H = 5{\cdot}9$, $z/H = 0{\cdot}041$; – – –, $z/H = 0{\cdot}083$; — —, $0{\cdot}250$; – – · – –, ES, $x/H = 1{\cdot}92$, $z/H = 0{\cdot}10$; — · —, $z/H = 0{\cdot}29$.

instrument was not affecting the energy-containing region of the spectra. No attempt has been made to remove any effects of intermittency from the spectra. Unlike velocity spectra, where irrotational fluctuations can contribute, the flat zero signal for the concentration will not of itself contribute to the spectra, although the on/off type of signal associated with the arrival of concentration pulses may in some cases be the dominant contribution. Figure 11 gives the vertical variation in spectral shapes at $x/H = 5{\cdot}92$, $y/H = 0$ for the GLS, and the vertical variation at $x/H = 1{\cdot}92$, $y/H = 0$ for the ES. Results for the ES, once the plume has become influenced by the ground, resemble those for the GLS. $E(k_1)$ is the one-dimensional wavenumber spectrum, with wavenumber $k_1 = 2\pi f/U$, U being the local flow speed. There is a narrow $-\frac{5}{3}$ region (inertial subrange) in these measurements which is much more limited than in the corresponding velocity spectra (see figure 2), especially at low wavenumber. It is possible to deduce the rate of dissipation of concentration fluctuations ϵ_c from a universal relationship for the inertial subrange (Bradshaw 1976):

$$E(k_1) = \text{const.} \times 2\epsilon_c \epsilon^{\frac{1}{3}} k_1^{-\frac{5}{3}}, \tag{2}$$

where ϵ is the rate of dissipation of turbulent-velocity fluctuations. The application of the above to highly intermittent signals is doubtful, although results shown later do not indicate a large error from this source. The estimated value of the Kolmogorov microscale of concentration $\eta_c = (D^3/\epsilon)^{\frac{1}{4}}$, was about $10^{-4}H$ ($\simeq 0{\cdot}1$ mm) and, as it is expected that molecular diffusion effects operate at scales of $10\eta_c$, and smaller, it follows that the lateral sensor dimension ($\simeq 1$ mm) are large enough to affect the

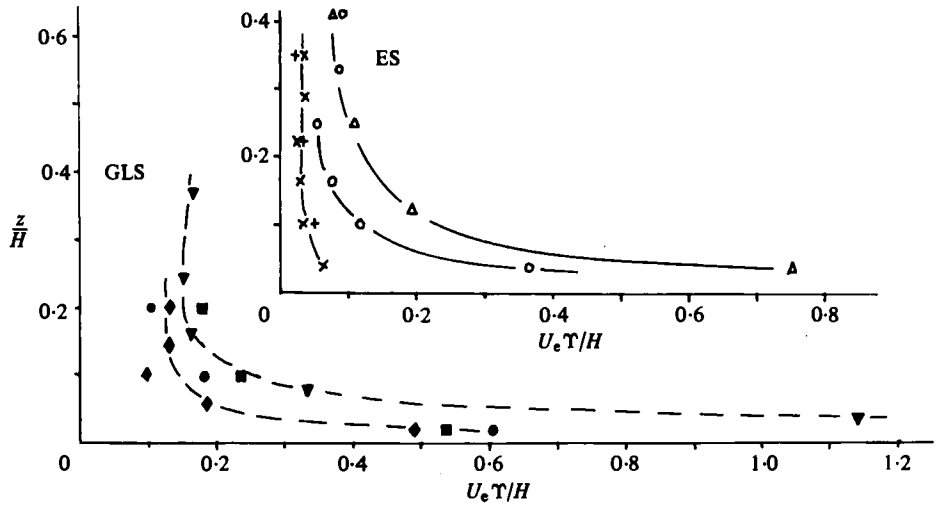

FIGURE 12. Integral time scales of concentration fluctuations: ◆, GLS, $z/H = 2{\cdot}50$, $y/\delta_v = 0$; ●, 2·50, 0·47; ■, 2·50, 1·07; ▼, 5·92, 0; ×, ES, 1·92, 0; +, 1·92, 0·96; ○, 3·83, 0; △, 6·52, 0.

observed spectra throughout the range of scales affected by molecular processes. On a wavenumber basis, $10\eta_c$ is equivalent to a dimensionless wavenumber $2\pi H/10\eta_c$ of about 7000. However, it is the instrumentation frequency response which sets the upper limit, since the -3 dB point is equivalent to a wavenumber of about 10^3. Although the high-frequency ranges of the observed spectra suffer from effects of inadequate instrument performance, it is clear from figure 11 that the entire 'energy-containing' range of scales is observed adequately in the present experiments. The greatest differences between the results for the two sources occur for the lower wavenumbers. The GLS results show a significant region prior to the $-\frac{5}{3}$ region ($k_1 H \simeq 3$–50) in which E fell at a somewhat slower rate (a slope of approximately $-1{\cdot}2$). The ES spectra fell even less rapidly in this wavenumber range (slope $\simeq -0{\cdot}7$), though the velocity spectra have a $-\frac{5}{3}$ slope. However, it should be noted (Bradshaw 1976) that the $-\frac{5}{3}$ slope for velocity spectra is frequently found at wavenumbers below those for which a 'universal equilibrium' concept should apply.

The ES results also show much less variation in integral scale (deduced from $E(k_1)$ for $k_1 \to 0$) than the GLS results, which is illustrated explicitly in figure 12, which shows the variation of the integral time scale Υ for both cases. The ES results for $x/H = 1{\cdot}92$ show only a slight variation across the plume both laterally and vertically. Moving further downstream, there is a general increase in scale, but the most noticeable effect is the great increase near to the ground. The results here exhibit the same form as the GLS results, which are similar at the two downstream positions measured and show little lateral variation. The corresponding spectra suggest that the relative increase in energy at low wavenumber, which increases the integral scale near the ground, is combined with reduced energy at medium wavenumber ($k_1 \simeq 5$–50). This may be because the small-scale eddies of the turbulent velocity field near the ground are relatively much more effective at mixing and destroying concentration fluctuations in this range than they are in dealing with the longer-term fluctuations associated with plume wandering. The overall energy $\overline{c^2}$ decreases near to the ground.

The time scale is given in figure 12, as opposed to the length scale, because of its

importance in connection with the time-averaging of concentration fluctuations. The measured fluctuations may be assumed to be effectively 'instantaneous', since the spectra show that there is very little energy at shorter times (higher wavenumbers) than the effective averaging time of the instrument. The discussion of Durbin (1980) is germane to this statement as the measured fluctuations are, strictly speaking, those defined by Durbin's 'outer limit'. However, in the application of the present results to practical situations, interest often lies in the level of fluctuations averaged over a given time. For example, for a plume of poisonous or noxious gas, the necessary averaging time is of the order of man's breathing cycle, or of sulphur dioxide a time associated with absorption by leaves of a given crop. The effect of time-averaging on the variance $\overline{c^2}$ is discussed in Pasquill (1974). For similar-shaped spectra and a given averaging time τ the variance $\overline{c_\tau^2}$ of the averaged data will be reduced least for a spectrum with a large integral time scale. As a rough guide, assuming an exponential autocorrelation gives

$$\overline{c_\tau^2}/\overline{c^2} = 2\frac{\Upsilon}{\tau}\left[1-\frac{\Upsilon}{\tau}(1-e^{-\tau/\Upsilon})\right].$$

As well as the variance, the overall shape of the p.d.f.s are altered by time-averaging the data. The occurrence of extreme and zero values is reduced with increased averaging time; γ increases, as does the ratio c_{99}/c'. Figure 12 shows that statistical quantities measured near the ground will be the least affected by any time averaging. Conversely, to obtain consistent mean values near the ground will require a longer overall sampling time, as is indeed observed.

5.4. *Transport equation*

The variance of the concentration fluctuations obeys a transport equation of the form

$$U\frac{\partial \overline{c^2}}{\partial x} + \underbrace{\left\{2\overline{uc}\frac{\partial C}{\partial x} + 2\overline{wc}\frac{\partial C}{\partial z} + 2\overline{vc}\frac{\partial C}{\partial y}\right\}}_{\text{(II)}} + \underbrace{\left\{\frac{\partial \overline{uc^2}}{\partial x} + \frac{\partial \overline{wc^2}}{\partial y} + \frac{\partial \overline{vc^2}}{\partial z}\right\}}_{\text{(III)}} + \underbrace{2\epsilon_c}_{\text{(IV)}} = 0, \qquad (3)$$

(I)

where

$$\epsilon_c = D\overline{\frac{\partial c}{\partial x_j}\frac{\partial c}{\partial x_j}},$$

and D is the molecular diffusion coefficient. Terms (I) to (IV) represent respectively advection of $\overline{c^2}$ by the mean velocity, generation by gradients in mean concentration, diffusion by turbulent-velocity fluctuations ($\gg$ molecular diffusion), and dissipation due to molecular diffusion of the fine-scale concentration fluctuations. All the quantities in this equation have been measured directly except the dissipation, which can therefore be obtained by difference, as well as deduced from spectra, as described earlier. Results showing the relative importance of the terms for two stations on the centre line of the ground-level plume and at 3 stations on the centre line of the elevated plume are given in figure 13. Except for the elevated case at $x/H = 1{\cdot}92$, where diffusion is important, the resultant balances are dominated by advection and dissipation. The production was found to be small relative to the advection in all the measurements (e.g. at $x/H = 1{\cdot}92$ it is between 1–10 % of the advection). Checks at positions off the centre line, where the production is increased by a $\partial C/\partial y$ term, still showed the advection term significantly larger. The near-source measurements for $\hat{c}/C_m$ given in figure 5 suggest that most of the production of $\overline{c^2}$ occurs very close to the source, and

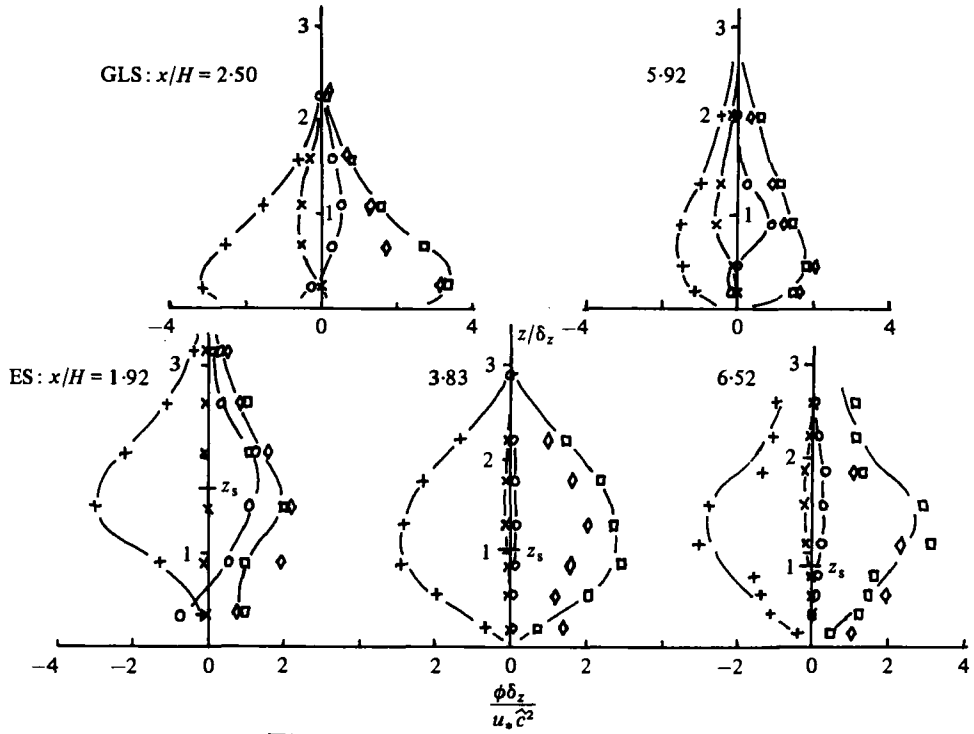

FIGURE 13. $\overline{c^2}$ balances: +, advection; ×, production; ○, diffusion; □, dissipation by difference; ◇, dissipation by spectra.

the overall level of the fluctuations is decaying thereafter. Indeed, the value of $\hat{c}^2\delta_y\delta_z$, roughly proportional to the integral of $\overline{c^2}$ over the plume, or the total flux of variance, decreases monotonically with increasing downstream distance from the nearest point of measurement, $x/H = 0{\cdot}21$. As the rate of change of the integrated flux is equal to the difference between the production and dissipation, i.e. the slender-plume form of (3) gives

$$\frac{d}{dx}\int_0^\infty\int_{-\infty}^\infty U\overline{c^2}\,dy\,dz + 2\int_0^\infty\int_{-\infty}^\infty\left(\overline{vc}\frac{\partial C}{\partial y}+\overline{wc}\frac{\partial C}{\partial z}\right)dy\,dz + 2\int_0^\infty\int_{-\infty}^\infty \epsilon_c\,dy\,dz = 0, \quad (4)$$

it can be seen that, downwind of a concentration-fluctuation-generation region extending to a few integral scales downstream, the behaviour is one of general decay, the initial level being determined by the source size to integral scale ratio. Results presented in Robins & Fackrell (1979) for a GLS in a different boundary layer suggest that very far downstream, $x/H \geqslant 20$, the relative importance of the production term may increase again to a similar magnitude to the advection. The dissipation still remains greater than production, but the rate of decrease of the level of fluctuations becomes smaller. Interestingly enough, the production term away from the immediate vicinity of the source is reasonably source-size-independent, at least for the cases studied, as inspection of the mean-concentration equation suggests.

Despite the small $-\frac{5}{8}$ region, the dissipation values obtained by difference and spectra in figure 13 are in approximate agreement, assuming that the constant in (2)

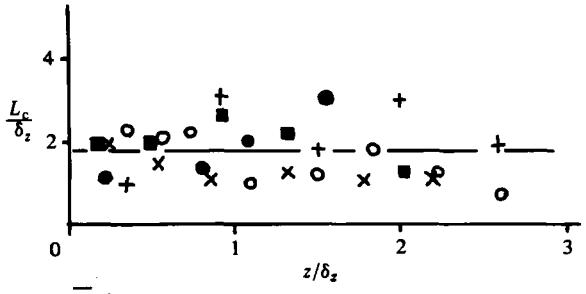

FIGURE 14. $\overline{c^2}$ dissipation length scale: ●, GLS, x/H = 3·0; ■, 5·92; +, ES, 1·92; ×, 3·83; ○, 6·52.

is 0·6. It can be seen that the dissipation decreases near the ground, in contrast to the case of high transfer to the boundary, when production and dissipation would both increase near the ground (like $1/z$). In order to model (3), the dissipation must be written in terms of known variables. A simple choice would be:

$$\epsilon_c = k^{\frac{1}{2}}\overline{c^2}/L_c, \tag{5}$$

where k is the energy of the turbulent-velocity fluctuations and L_c is a suitable length scale. Figure 14 shows values obtained for L_c/δ_z in the plumes for both sources and, although there is considerable scatter, the value is typically 2 and there is no obvious variation with fetch and height. Proportionality to δ_z implies that L_c becomes constant far downstream in a boundary-layer flow, but otherwise the time scale of the dissipation, $L_c/k^{\frac{1}{2}}$, grows with fetch, as suggested by Csanady (1967). As the ratio L_c/δ_z is similar in both plumes, it is to be expected that it is also source-size-independent. It is interesting to note that if (5) has universal applicability then the possibility exists far downwind for a local equilibrium to exist between production and dissipation, as follows from (4).

6. Concentration fluxes

6.1. *Fluxes and diffusivities*

As may be deduced from the transport equation applicable to a two-dimensional turbulent boundary-layer flow, viz

$$U\frac{\partial C}{\partial x}+\frac{\partial \overline{wc}}{\partial z}+\frac{\partial \overline{vc}}{\partial y}=0, \tag{6}$$

it is the magnitude of the turbulent fluxes $\overline{wc}$ and $\overline{vc}$ which determines the rate of spread of the plume in the vertical and horizontal. Yet, despite their importance, there have been very few reports of turbulent-scalar-flux measurements related directly to the present study. Most measurements that have been made are of heat fluxes in cases with high heat transfer to or from the wall and, as already indicated, a passive scalar with no transfer is a significantly different situation. It follows directly from (6) that since the mean-concentration field, away from the immediate vicinity of the source, is source-size-independent so must be the turbulent fluxes $\overline{wc}$ and $\overline{vc}$.

Figure 15 shows $\overline{wc}$ values for the GLS at two plume stations (N.B., in the figure C_m is the local maximum concentration for each profile). If the vertical profiles were self-

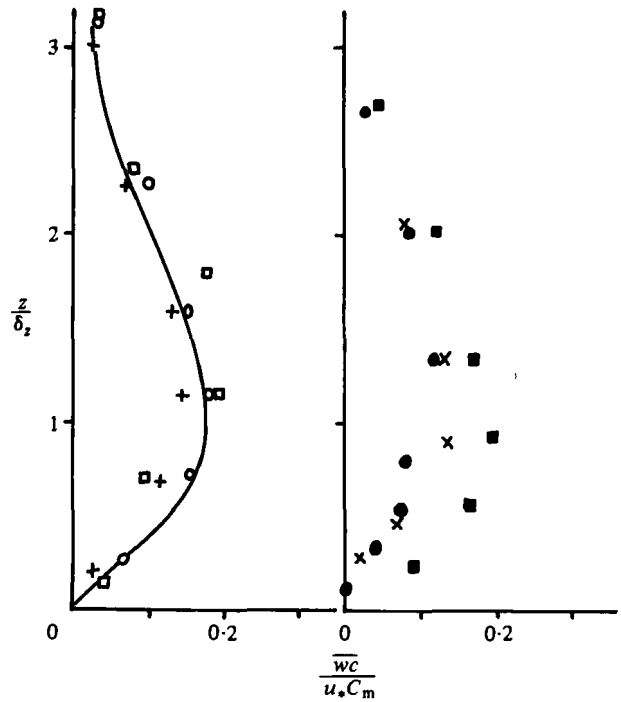

FIGURE 15. Vertical flux, $\overline{wc}$, GLS: ×, $x/H = 5{\cdot}92$, $y/\delta_y = 0$; ●, 5·92, 0·51; ■, 5·92, 1·20; +, 2·50, 0; ○, 2·5, 0·39; □, 2·5, 1·07; ——, $\overline{wc}$ by integration.

similar across the plume and $\overline{wc}$ varied laterally in the same way as the mean concentration, then the profiles as plotted should collapse on one another. They in fact show some variation in magnitude, but not in shape, though, as the variation is not consistent between the two stations, it may well be due to scatter in the data. If it is assumed that the conditions stated above are satisfied, it is shown in Robins & Fackrell (1979) that $\overline{wc}$ can then be derived from the mean-concentration values; indeed all the values of vertical turbulent flux in Robins & Fackrell were obtained in this way. When the same procedure is applied to the present results at $x/H = 2{\cdot}5$, the curve shown in figure 15 is produced. Bearing in mind the likely errors in this calculation, there is fairly good agreement with the direct measurements. The usual first-order closure of (6) models $\overline{wc}$ as $-\kappa_z \partial C/\partial z$, with eddy diffusivity proportional to the eddy viscosity ν_t. Both the derived results in Robins & Fackrell and the present results for the GLS agree with this formulation provided that ν_t/κ_z is approximately 0·8. It is to be expected that the vertical flux for the GLS can be modelled in this way, since the eddies responsible for the spreading are the same size or smaller than the plume.

The variation with downstream distance of the vertical flux on the centre line of the plume from the ES is shown in figure 16. The flux profiles develop from being anti-symmetric about the source height near the source, towards a ground-level-source profile. The later profiles show very low values over the bottom part of the plume, corresponding to the fairly constant value of mean concentration (figure 4). The rough correspondence between maxima and zeros in $\overline{wc}$ and $\partial C/\partial z$ suggests that a gradient-transfer model for $\overline{wc}$ may be appropriate. However, because for the ES the vertical

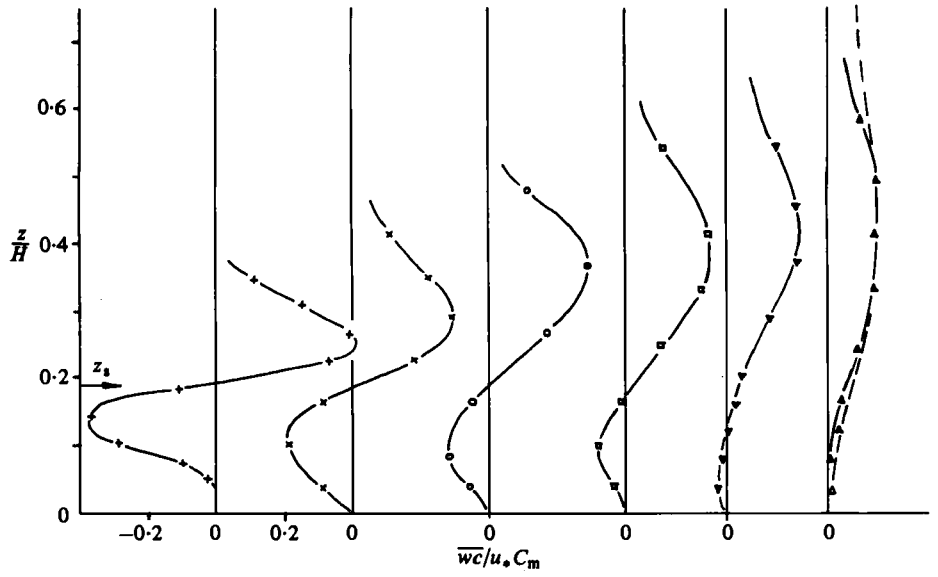

FIGURE 16. Vertical flux, $\overline{wc}$, ES, $y/H = 0$: +, $x/H = 0{\cdot}96$; ×, 1·92; ○, 2·88; □, 3·83; ▽, 4·79; △, 5·62. – – –, GLS result.

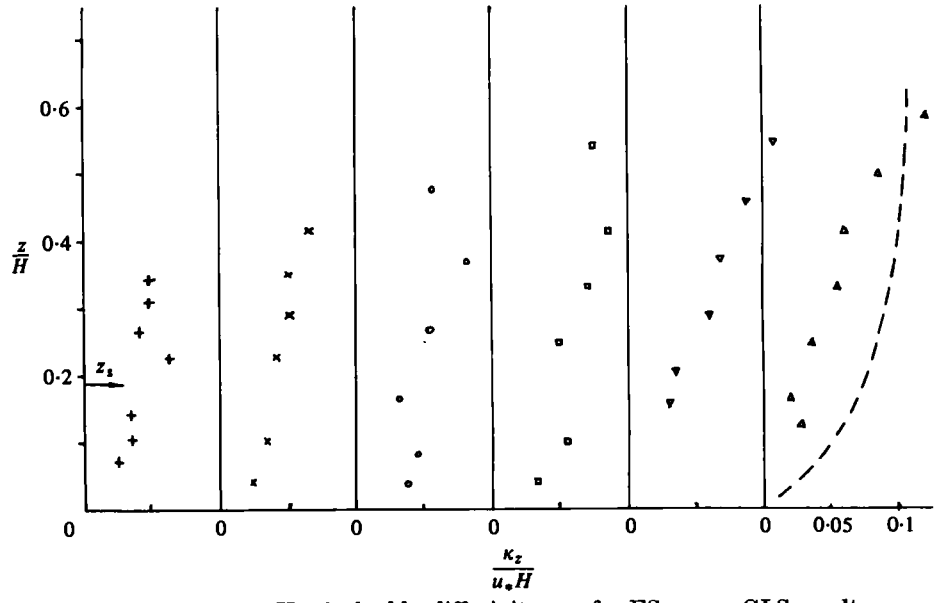

FIGURE 17. Vertical eddy diffusivity, κ_z, for ES. – – –, GLS result. Symbols as in figure 16.

eddies are not limited to the plume size, the eddy diffusivity must be a function of distance from the source. Derived values of eddy diffusivity κ_z, given in figure 17, exhibit the expected increase in value with downstream distance, except for the last profile, which appears to show a decrease in the lower portion of the profile. This, most likely, reflects the error in deriving the eddy diffusivity when both $\overline{wc}$ and $\partial C/\partial z$ are small. The profile of diffusivity for the GLS is also indicated in the figure. Near the

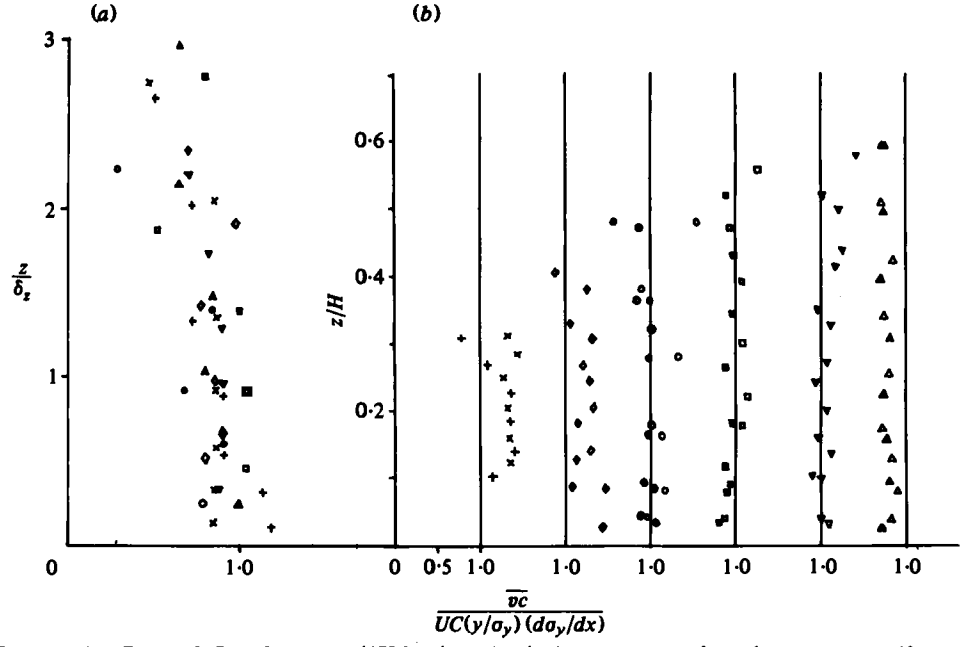

FIGURE 18. Lateral flux $\overline{vc}$, as $\overline{vc}/\{UC(y/\sigma_y)\,d\sigma_y/dx\}$. (*a*) GLS: ◇, $x/H = 0{\cdot}83$, $y/\delta_y = 1{\cdot}59$; □, 0·83, 0·67; △, 2·50, 1·07; ○, 2·50, 0·39; ▽, 4·17, 1·04; ×, 5·92, 0·33; +, 5·92, 0·14. (*b*) ES: +, $x/H = 0{\cdot}96$, $y/\delta_y = 0{\cdot}59$; ×, 0·96, 1·26; ◇, 1·92, 0·36; ◆, 1·92, 0·96; ○, 2·88, 0·36; ●, 2·88, 0·89; ◐, 2·88, 1·27; □, 3·83, 0·90; ■, 3·88, 1·43; ▽, 4·79, 0·75; ▼, 4·79, 1·34; △, 6·52, 0·69; ▲, 6·52, 1·14.

surface, $\overline{wc}$ tends to zero, since there is no mass transfer through the surface, and it is found that the 'structure function' $\overline{wc}/(-\overline{uv})^{\frac{1}{2}}c'$ also tends to zero at the ground, as shown in Robins & Fackrell for the GLS.

Within experimental error it has been found that the lateral profiles of mean concentration at any downstream station are similar and independent of z. This suggests that $C = C(x,z)f(\eta)$, where $\eta = y/\sigma_y$ and $\sigma_y = \sigma_y(x)$. In addition, the results for $\overline{wc}$ indicate that its lateral variation is closely similar to that of the mean concentration, so that writing $\overline{wc} = \widetilde{wc}(x,z)f(\eta)$ should be a reasonable approximation. As shown in Robins & Fackrell, if these expressions are substituted into (6), an expression is obtained for the lateral flux at any position:

$$\overline{vc} = UC\frac{y}{\sigma_y}\frac{d\sigma_y}{dx}. \tag{7}$$

If the function $f(\eta)$ is Gaussian, as the results suggest, and an eddy-diffusivity form for $\overline{vc}$ is used, then (7) implies further that the eddy diffusivity κ_y obeys the relation

$$\kappa_y/U = \frac{1}{2}\frac{d\sigma_y^2}{dx} \quad \text{(i.e. a function of } x \text{ only)}. \tag{8}$$

This is the same expression as that obtained from statistical theory for dispersion in a uniform wind, except that in the present case U varies with height. Equations (7), and by implication (8), have been tested for the GLS and ES in figure 18. Although there is some scatter, allowing for likely errors, the results provide fairly good confirmation of (7); in particular, the results at each station are quite uniform with height.

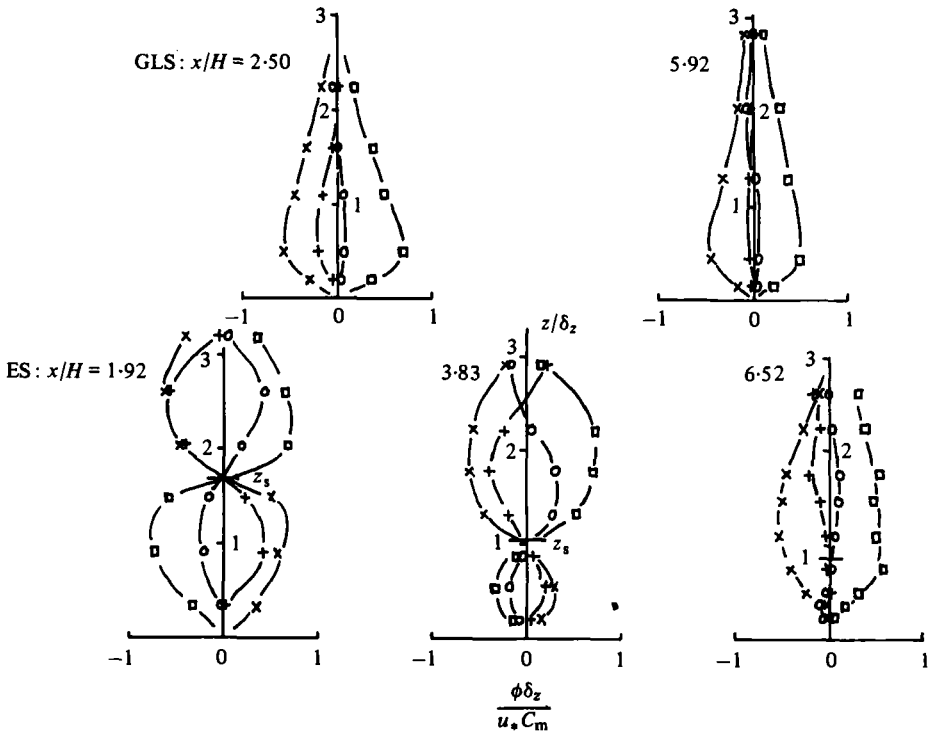

FIGURE 19. Vertical flux balances, $y/H = 0$: +, advection; ×, production; ○, diffusion; □, difference.

6.2. *Transport equations*

There is an increasing trend towards the use of 'second-order modelling' in the calculation of turbulent dispersion, i.e. the modelling of transport equations for the fluxes themselves. It is hoped in this way to account for the advection and diffusion of the fluxes and so make a given calculation set more generally valid, as has been attempted with regard to the turbulent stresses. The transport equation for the vertical flux $\overline{wc}$, as applied to the present two-dimensional boundary-layer flow, is

$$U\frac{\partial \overline{wc}}{\partial x} + \left(\overline{uw}\frac{\partial C}{\partial x} + \overline{w^2}\frac{\partial C}{\partial z}\right) + \left(\frac{\partial}{\partial x}\overline{uwc} + \frac{\partial}{\partial z}\overline{w^2 c} + \frac{\partial}{\partial z}\frac{\overline{p'c}}{\rho}^{(*)}\right) + \varepsilon_{wc}^{(*)} - \frac{\overline{p'}}{\rho}\frac{\partial c}{\partial z}^{(*)} = 0. \quad (9)$$

(I) (II) (III) (IV) (V)

Terms (I)–(V) represent respectively advection, production, diffusion due to turbulent velocity and pressure fluctuations, dissipation, and a pressure–concentration-gradient correlation that acts to limit the growth of the fluxes. With the present measurement system it is not possible to measure those terms marked by an asterisk, and they have been lumped together as a difference term to balance the equation. It is expected that term (V) will make by far the dominant contribution to this difference term and henceforth the two will be treated as being identical (see e.g. Launder 1976). Results for two stations on the centre line of the GL plume are given in figure 19. At both stations, a balance between production and the difference term dominates; advection and diffusion being much smaller. The main contribution to the production term is from

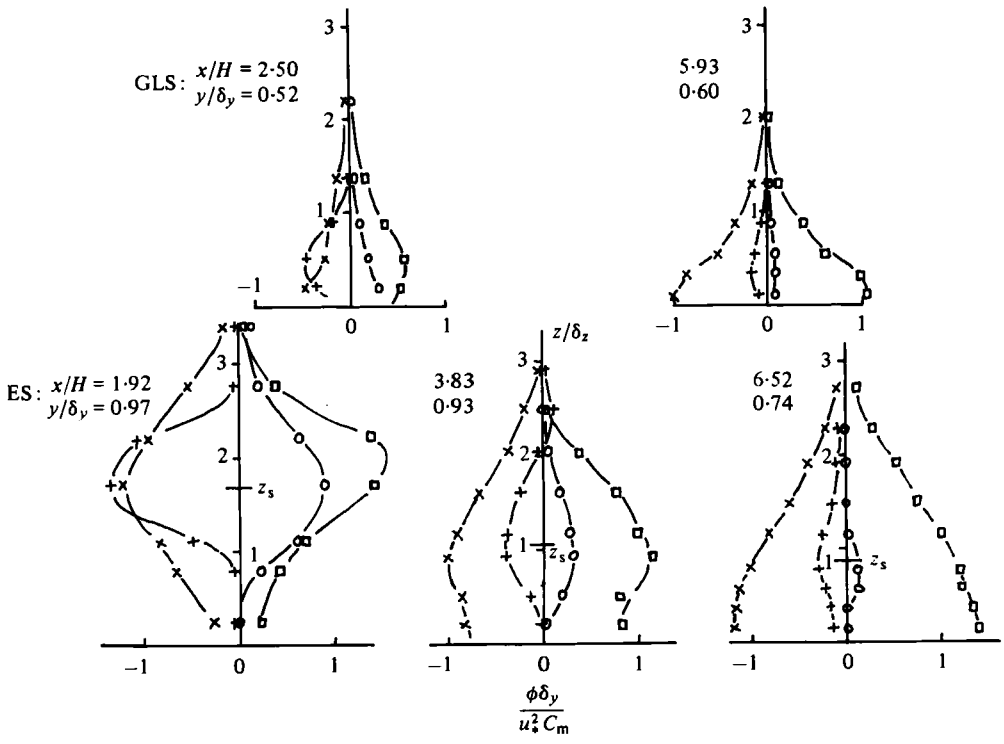

FIGURE 20. Lateral flux balances. Symbols as for figure 19.

$\overline{w^2}\,\partial C/\partial z$ and that to the diffusion term is from $\partial\overline{w^2c}/\partial z$. Also shown are $\overline{vc}$ balances for the ES at 3 downstream stations on the plume centre line and in this case, near to the source, advection and diffusion are the same order as the other terms, only becoming much smaller at the furthest downstream position.

A transport equation for the lateral flux $\overline{vc}$ can also be derived:

$$U\frac{\partial\overline{vc}}{\partial x}+\left(\overline{uv}\frac{\partial C}{\partial x}+\overline{v^2}\frac{\partial C}{\partial y}\right)+\left(\frac{\partial}{\partial x}\overline{uvc}+\frac{\partial}{\partial y}\overline{v^2c}+\frac{\partial}{\partial y}\frac{\overline{p'c}}{\rho}^{(*)}\right)+\epsilon_{vc}^{(*)}+\frac{\overline{p'}}{\rho}\frac{\partial\overline{c}^{(*)}}{\partial y}=0, \quad (10)$$

(I) (II) (III) (IV) (V)

where the numbered terms represent the same physical processes as in (9) and the asterisks indicate terms that were not measured. The $\overline{vc}$ balances obtained for the GLS and ES plumes are given in figure 20. In both cases, there is an approximate balance between production and the difference terms only at the position furthest from the source. Closer to the source, the diffusion and, in particular, the advection become equally important.

Some measurements of the triple-product terms occurring in the flux-transport equations are presented in figure 21. The accuracy of the data precludes evaluation of the diffusion coefficients implied in the gradient-transport modelling of these terms, though evaluations of $\overline{w^2c}$ from $\kappa_z\,\partial\overline{wc}/\partial z$, with the appropriate κ_z taken from figure 17, are shown. This comparison is inconclusive, as similar agreement could have been obtained by using a suitable constant value of κ_z. Nonetheless, whenever plume dimensions are significantly less than the local turbulence scales it is to be expected

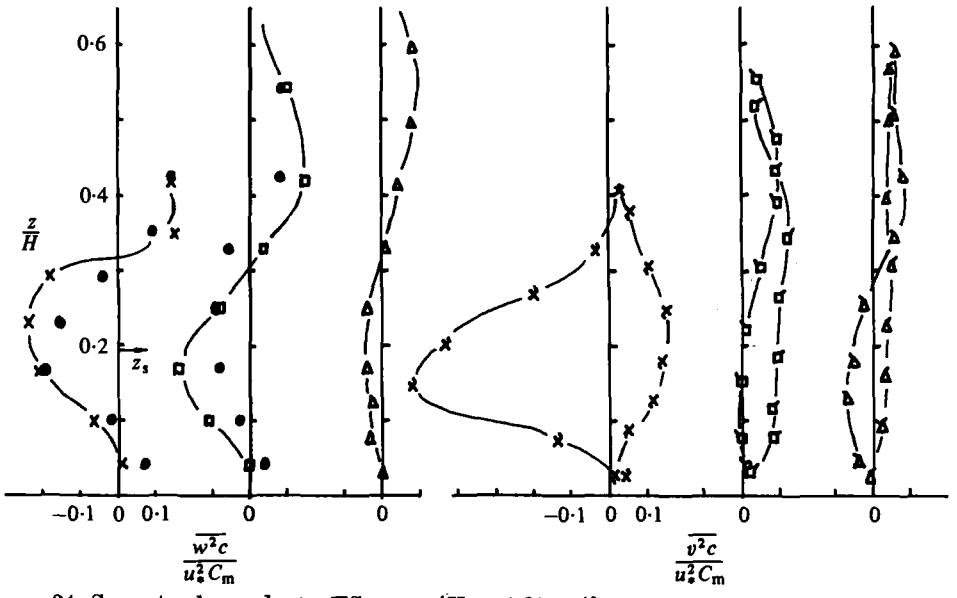

FIGURE 21. Some triple products, ES: ×, $x/H = 1{\cdot}92$, $y/\delta_y = 0$; ×, 1·92, 0·36; ×, 1·92, 0·96; □, 3·83, 0; □, 3·83, 0·90; □, 3·83, 1·43; △, 6·52, 0; △, 6·52, 0·69; △, 6·52, 1·14; ●, $-(\kappa_z/u_*^2 C_m)\,\partial\overline{wc}/\partial z\,\overline{wc}$.

that any diffusion coefficient is fetch-dependent, as has been demonstrated by Deardorff (1978) by comparing predictions of first-, second- and third-order models of plume dispersion. Similar comments apply to 'convection-velocity' modelling of the form

$$\overline{w^2c} \sim w_c \overline{wc},$$

where w_c is the convection velocity. Whichever approach is made, account must be taken of the scale differences between the plume and the surrounding turbulence field. From figures 19 and 20 it can be seen that where advection and diffusion are important (i.e. near the source) they are almost equal and opposite and, hence, reasonably accurate modelling of the diffusion is required.

Finally, it is perhaps worth while to comment on one or two matters which arise from the flux-transport equations. Generally speaking, whenever a balance prevails between the production and the pressure–concentration-gradient correlation terms a fetch-independent, eddy-diffusivity behaviour is expected to result. For example, if in (10) the latter term is modelled as vc/T_y, then it follows that $vc = -\overline{v^2}T_y\partial C/\partial y$, a result which also follows from statistical theory, with T_y a Lagrangian time scale. It is often assumed (e.g. Pasquill 1974) that Lagrangian and Eulerian scales are related as $T_y = \alpha L_y/v'$, where α is a constant and L_y the Eulerian length scale. Combining this with (7) and (8) gives

$$\kappa_y = U\sigma_y\, d\sigma_y/dx = \overline{v^2}T_y = \alpha v' L_y,$$

which implies that, to a first approximation, the length scales $\overline{v^2}T_y/U$ and $v'L_y/U$ are independent of height. It is worth noting that the present results suggest $\alpha = 0{\cdot}8$, which is somewhat greater than the usually assumed value of about 0·5.

7. Conclusions

The aim of this paper has been to explore the behaviour of concentration fluctuations and fluxes in slender plumes from point sources. Comparatively little attention has been given to the mean concentration field – this has been deliberate and such treatments may be found elsewhere (e.g. Shlien & Corrsin 1976; Robins & Fackrell 1979).

It has been shown that most of the fluctuations are produced very near to the source, and that the maximum level attained is strongly source-size-dependent. The general level of fluctuation then decays in line with an approximate balance between advection and dissipation, except perhaps far downstream, where production may also be important. If the dissipation is modelled as $k^{\frac{1}{2}}\overline{c^2}/L_c$, then L_c is a fixed fraction of the vertical plume width. Thus the time scale of dissipation $L_c/k^{\frac{1}{2}}$ increases with downstream distance, as does the integral scale of the fluctuations. A general model, applicable to cases of zero and non-zero surface transfer, would clearly require a more sophisticated handling of the dissipation. The condition of no transfer at the ground has a pronounced influence on the nature of the concentration fluctuations as the mean-square c^2 decreases towards zero and the integral scale increases near the ground. The p.d.f.s change from an 'exponential' form towards a more Gaussian one, with increasing values of intermittency factor γ. However, despite these different forms, the peak concentration ratio c_{gg}/c' remains fairly constant at about 4·5.

Since the fluxes determine the behaviour of the mean-concentration profile, which away from the immediate vicinity of the source is observed to be source-size-independent, it follows that the fluxes themselves must be independent of the source size. The vertical flux $\overline{wc}$ has a self-preserving form for the GLS, and can be modelled by the eddy-diffusion approximation with $\nu_t \simeq 0{\cdot}8\kappa_z$. For the elevated source, κ_z shows an increase with distance from the source, and this is associated with the advection and diffusion of $\overline{wc}$. Lateral profiles of $\overline{uc}$ follow the Gaussian profiles of the mean concentration, with the spread σ_y a function of x only. This leads to the lateral flux $\overline{vc}$ behaving like $(UCy/\sigma_y)\,d\sigma_y/dx$, and hence $\kappa_y/U = \frac{1}{2}\,d\sigma_y^2/dx$, for both of the sources studied. The downstream variation of κ_y is again associated with the advection and diffusion terms in the flux-transport equations.

Examination of the flux-transport equations shows that, far downstream, there is an overall balance between production and the $\overline{(p'/\rho)\,(\partial c/\partial x_i)}$ term, and this leads to an eddy diffusion form for the flux. In general, near to the source, the advection and diffusion terms are of similar magnitude to the above terms, and consequently reasonably accurate modelling of the triple-product terms must be undertaken. This poses problems, essentially because the plume to turbulence length scale ratio is fetch-dependent. This is the same problem that exists for first-order, or eddy-diffusivity, modelling. Consequently, there may not be a great deal to gain from second-order modelling in the case of a passive plume in an undisturbed boundary layer, as Deardorff (1978) has also shown for homogeneous turbulence, though it may be advantageous in more complex flow situations. In such high-order modelling it must be recognized that fluctuations, unlike fluxes, are strongly source-size-related, and thus it is unlikely that they should play any significant role in the modelled flux equations.

As for the future, there is clearly a need for further experimentation, in particular

in the concentration-fluctuation-generation region. The effects of turbulence level and scale also require attention, as do the consequences of imperfect instrument response. Of course, such work should go hand in hand with the development of more refined modelling techniques.

We would like to acknowledge helpful discussions with Drs A. Nakayama and P. Bradshaw of Imperial College during the course of a C.E.G.B. contract on 'Turbulent plume dispersion'. The work reported here was carried out at Marchwood Engineering Laboratories and is published by permission of the Central Electricity Generating Board.

REFERENCES

Barry, P. J. 1970 *A.E.C.L. Rep.* no. 3731.

Becker, H. A., Rosensweig, R. E. & Gwozoz, J. R. 1966 *A.I.Ch.E. J.* **12**, 964–972.

Belorgey, M., Nguyen, A. D. & Trinite, M. 1979 Diffusion from a line source in a turbulent boundary layer with transfer to the wall. In *Proc. 2nd Symp. on Turbulent Shear Flows, Imperial College, London.*

Birch, A. D., Brown, D. R., Dodson, M. G. & Thomas, J. R. 1978 *J. Fluid Mech.* **88**, 431–449.

Bradshaw, P. 1976 In *Turbulence* (ed. P. Bradshaw), pp. 1–44. Springer.

Chatwin, P. C. & Sullivan, P. J. 1979 *J. Fluid Mech.* **91**, 337–355.

Counihan, J. 1969 *Atmos. Env.* **3**, 197–214.

Csanady, G. T. 1967 *J. Atmos. Sci.* **24**, 21–28.

Deardorff, J. W. 1978 *Phys. Fluids* **21**, 525–530.

Durbin, P. A. 1980 *J. Fluid Mech.* **100**, 279–302.

Fackrell, J. E. 1978 *C.E.G.B. Res. Note* R/M/N1016.

Fackrell, J. E. 1980 *J. Phys.* E, *Sci. Instrum.* **13**, 888–893.

Fackrell, J. E. & Robins, A. G. 1982 *Boundary-Layer Met.* (to be published).

Freymuth, D. & Uberoi, S. 1973 *Phys. Fluids* **16**, 161–168.

Gad-el-Hak, M. & Morton, J. B. 1979 *A.I.A.A. J.* **17**, 558–562.

Gifford, F. A. 1959 *Adv. Geophys.* **6**, 117–137.

Harter, C. A., Kaiser, G. D., Goddard, A., Gosman, A. D., Ghobadian, A. & El Tahry, S. 1980 In *Proc. C.E.C. Seminar on Radioactive releases and their dispersion in the atmosphere, Riso, Denmark.*

Hay, J. S. & Pasquill, F. 1959 *Adv. Geophys.* **6**, 345–365.

Hunt, J. C. R. & Weber, A. H. 1979 *Quart. J. R. Met. Soc.* **105**, 423–443.

Jones, C. D. 1979 In *Mathematical Modelling of Turbulent Diffusion in the Environment* (ed. C. J. Harris), pp. 277–298. Academic.

Launder, B. E. 1976 In *Turbulence* (ed. P. Bradshaw), pp. 232–287. Springer.

Lewellen, W. S. & Teske, M. E. 1976 *Boundary-Layer Met.* **10**, 69–90.

O'Brien, E. E. 1978 *J. Fluid Mech.* **89**, 209–222.

Pasquill, F. 1974 *Atmospheric Diffusion.* Ellis-Horwood.

Robins, A. G. 1978 *Atmos. Env.* **12**, 1033–1044.

Robins, A. G. 1979 *J. Ind. Aero.* **4**, 71–100.

Robins, A. G. & Fackrell, J. E. 1979 In *Mathematical Modelling of Turbulent Diffusion in the Environment* (ed. C. J. Harris), pp. 55–114. Academic.

Shlien, D. H. & Corrsin, S. 1976 *Int. J. Heat Mass Transfer* **19**, 285–295.

Smith, F. B. & Hay, J. S. 1961 *Quart. J.R. Met. Soc.* **87**, 82–91.

Thomas, J. R. 1979 In *Mathematical Modelling of Turbulent Diffusion in the Environment* (ed. C. J. Harris), pp. 33–53. Academic.